# Unconstrained $\ell_1-$Regularized Minimization with Interpolated Transformations for Heart Motion Compensation

Angelica I. Aviles[1], Pilar Sobrevilla[2] and Alicia Casals[3]

***Abstract*— Motion compensation constitutes a challenging issue in minimally invasive beating heart surgery. Since the zone to be repaired has a dynamic behaviour, precision and surgeon's dexterity decrease. In order to solve this problem, various proposals have been presented using $\ell 2$-norm. However, as they present some limitations in terms of robustness and efficiency, motion compensation is still considered an open problem. In this work, a solution based on the class of $\ell 1-$Regularized Optimization is proposed. It has been selected due to its mathematical properties and practical benefits. In particular, deformation is characterized by cubic B-splines since they offer an excellent balance between computational cost and accuracy. Moreover, due to the non-differentiability of the functional, the logarithmic barrier function is used for generating a standard optimization problem. Results have provided a very good trade-off between accuracy and efficiency, indicating the potential of the proposed approach and proving its stability even under complex deformations.**

## I. INTRODUCTION

In the last years, minimally invasive beating heart surgery has received much attention due to the well-known benefits ([1], [2]) that it can offer in contrast with traditional cardiac procedures. However, since the heart is not stopped during the operation, the surgeon has to deal with a dynamic target in which two perturbations are acting: heartbeat and breathing. They undertake the necessary precision surgery and compromise surgeon's dexterity. Therefore, a research ambition is to compensate them so that surgeons can get the feeling of working in a static area. The complexity of this problem increases due to the small workspace, variable light, heart characteristics (i.e. deformable, glossy surface) and the real time requirements. In addition, there exists a hardware limitation since the camera integrated in the endoscope is the most practical sensor to be used due to the space constraint. Due to all these difficulties, motion compensation in surgical applications still remains an open problem [3].

To overcome the aforementioned difficulties Lemma et al. [4] proposed a solution based on mechanical stabilization, using small devices positioned over the heart, for keeping the region to be repaired in steady state. However, they concluded that after mechanical stabilization there is significant residual coronary artery motion. Thus, a feasible solution is the use of Computer Vision Techniques (CVT). In this context, the first proposal that uses CVT was due to Nakamura et al. [5]. The authors introduced the concept of heart synchronization and made use of artificial markers for tracking the heart motion. Since the use of artificial markers is not feasible due to the difficulty of putting them over the heart surface, Ortmaier et al. [6] introduced the use of natural markers. In that work an affine tracking was proposed and simplified to a matching algorithm.

In [7] the problem of heart motion estimation was addressed in terms of displacement and acceleration by using calibrated landmarks placed on the heart surface, and then applying a texture based approach to avoid the use of such landmarks. Additionally, in [8] a combination of thin-plate splines and efficient second-order minimization were put forward as solution to this problem. In [9] authors suggested the combination of LK optical flow method and SURF for features detection. In [10] a tracking based on feature points was presented. These features were extracted via local maxima of the intensity.

A common factor of previous solutions is the use of the $\ell 2$-norm. Motivated by the current limitations of existing proposals and with the main objective to increase robustness and efficiency, in this work we propose a solution based on the $\ell 1$-norm. Particulary, our proposal uses the class of $\ell 1$-Regularized Optimization. In here, explicit regularization is employed in order to diminish the number of local minima, deal with the ill-posed problem and stabilize the system.

This paper is organized as follows: In Section II the presentation of the problem is tackled, the proposed solution is described in Section III. In Section IV, the results are presented, concluding with a discussion in Section V.

## II. PROBLEM DESCRIPTION

For tackling the heart motion compensation problem, a solution composed of four main modules is proposed. They are represented in Fig. 1. Particulary, this work focuses on the *heart motion module* (blue module). In here, the problem is treated as an energy minimization, in which two images are involved at each time instant; the reference image $I_F : \Omega_{I_F} \rightarrow \mathbb{R}$, and the acquired image $I_A : \Omega_{I_A} \rightarrow \mathbb{R}$, where the bounded domain is given by $\Omega_{I_A,I_B} \in \mathbb{R}^d$. Thus, the goal is to find the transformation depending on the displacement field, $u$, such that, $I_A(u) \sim I_F$. That is, the generalized problem is

*This work was supported by a FPU national scholarship from the Spanish Ministry of Education with reference AP2012-1943

[1] A.I. Aviles is with the Intelligent Robotics and Systems Group, Universitat Politècnica de Cataluya, 08034, Barcelona, Spain. angelica.ivone.aviles@upc.edu

[2] P. Sobrevilla is with the Department of Applied Mathematics II, Universitat Politècnica de Cataluya, 08034, Barcelona, Spain. pilar.sobrevilla@upc.edu

[3] A. Casals is with the Institute for Bioengineering of Catalonia and with the Universitat Politècnica de Cataluya, 08028, Barcelona, Spain. alicia.casals@upc.edu

978-1-4244-7929-0/14/$26.00 ©2014 IEEE

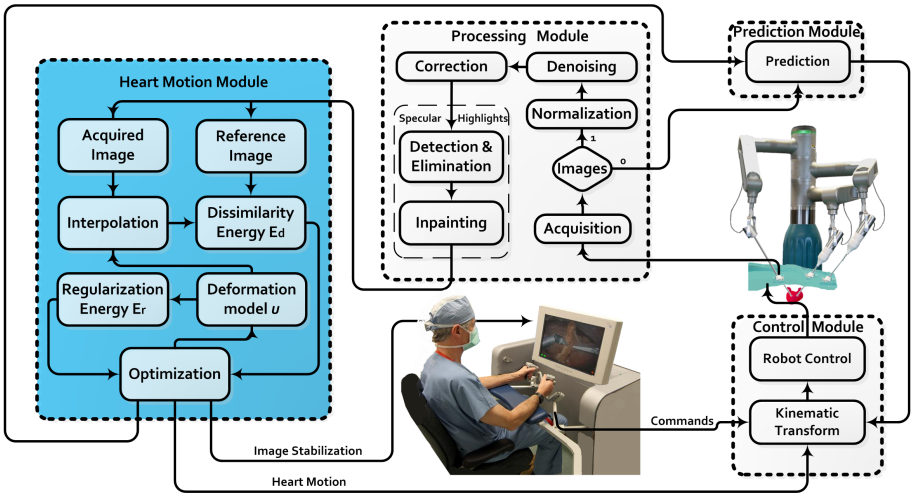


Fig. 1: Proposed scheme for heart motion compensation in a Robotic Surgical System.

described by

$$\min_u E_t(u) = \min_u \{E_d(I_A(u(x)+x), I_F(x)) + \gamma E_r(u(x))\} \quad (1)$$

where $E_t$ is the total energy, $E_d$ is the dissimilarity functional that allows measuring the level of alignment between the two images, and $E_r$ represents the regularization term used to obtain a plausible transformation. Moreover, $\gamma$ offers a balance between $E_d$ and $E_r$, and $x$ is a vector in $\mathbb{R}^d$.

## III. PROPOSED SOLUTION

In this section, the proposed solution for Eq. 1 is explained. It is based on the $\ell 1$-Regularized Optimization Class. It has been chosen due to its mathematical properties that provide good practical results. To our best knowledge this class has not been tested for solving this problem.

### A. Parametrization of the Displacement Field

In order to describe heart motion, it is necessary to select an adequate deformation model. Although there are different options, for this application, it has to be carefully selected since it is a real-time oriented problem, in consequence, short computational time and valuable information are highly desired [11]. Specially, in medical applications well-known models such as radial basis functions, elastic body, viscous fluid flow or statistical deformation models have been used. However, they have various drawbacks such as inverse inconsistency, lack of mathematical optimality, high computational cost or lack of efficiency dealing with complex deformations. Because these factors, cubic B-splines (free-forms) have been selected. They demand low running time, are easy to manipulate, allow multiresolution, have optimal mathematical properties and the capacity of keeping affine invariance [12].

The idea is to define a region of interest, $\mathrm{r_{int}} \subset \Omega$, delimited by a lattice, and describe the deformation in $\mathrm{r_{int}}$ via repercussion of each lattice point. Defining $\mathbf{P}$ as the set of control points, the displacement field is described by the following parametric domain

$$\begin{aligned} u(x) &= \sum_{j_1=0}^{n} \cdots \sum_{j_d=0}^{n} \mathbf{P}_{j_1,\ldots,j_d} \prod_{l=1}^{d} \beta_l(u_l) : \{u \in \mathbb{R}^d(\mathrm{r_{int}})\} \\ &= \sum_{l=0}^{3}\sum_{m=0}^{3} \beta_l(\mu)\beta_m(v)\mathbf{P}_{i+l,j+m} : \{u \in \mathbb{R}^2(\mathrm{r_{int}})\} \end{aligned} \quad (2)$$

with b-splines of degree $n$ and $d$-dimensions; $\beta_l$ and $\beta_m$ are basis function defined as

$$\begin{aligned} \beta_0(\mu) &= (1-\mu)^3/6\ , \quad \beta_1(\mu) = (4+3\mu^3-6\mu^2)/6 \\ \beta_2(\mu) &= (1-3\mu^3-3\mu^2+3\mu)/6\ , \quad \beta_3(\mu) = \mu^3/6 \end{aligned} \quad (3)$$

### B. Solution Description

To solve Eq. 1, firstly, it is necessary to evaluate the discrepancy between the two images. Although different methods can be considered, the selection of the most adequate depends on the problem to be solved. In here, since the images are acquired by the same sensor, big intensity variations between them are not expected. Therefore, an iconic method is a perfect match for this application. In particular, to reformulate $E_d$, the Sum of Absolute Differences (SAD) method has been selected for its simplicity, low computational time working in real-time, and robustness in front of variation of intensities and outliers.

Secondly, as undesirable mathematical properties appear, they lead us to deal with an ill-posed problem. This kind of problem is characterized by the fact that it does not fulfill the Hadamards postulate [13], which asserts that a well-posed problem must satisfy three main requirements: i) existence, ii) uniqueness and iii) continuity. Thus, it is necessary to define the penalization term, $E_r$, in order to impose stability to the solution and decrease the number of local minima.

There are different options for $E_r$ such as the classic method called Tikhonov, the Mumford and Shah model, curvature, among others. However, some problems such as lack of edge preservation, complex analysis or negative practical results lead us to select the method proposed by Rudin et al. called Total Variation (TV) [14]. It has been

chosen due to its performance in edge preservation, its easy interpretation and analysis, and its short computational time. Reformulating Eq. 1 using both TV and SAD methods, the above functional becomes

$$E_t(u) = \underbrace{\frac{1}{2}\int_\Omega |I_A(u(x)+x) - I_F(x)|dx}_{Ed} + \underbrace{\gamma \sum_{d=1}^{n} \int_\Omega |\nabla u_d(x)|dx}_{Er} \tag{4}$$

where $\nabla u = (\frac{\partial u}{\partial x_1}, \frac{\partial u}{\partial x_2} \cdots \frac{\partial u}{\partial x_N})$.

### C. The Discretize-Optimize Approach

From a practical point of view and efficiency, in this work the discretize-then-optimize methodology is used. Strictly speaking, taking original continuous functional from Eq. 4, it is rewritten by a discretization in order to obtain a standard optimization problem. Despite all desired mathematical and practical properties of the $\ell_1-$ class, the main challenge for solving Eq. 4 relies on its nondifferentiability, which hinders the optimization process. To handle this inconvenience, different alternatives can be followed, such as: subgradient and subderivatives methods, rewrite this problem as a constraint optimization or substitute the original functional by a differentiable approximation. The first two alternatives tend to have a slow convergence, sometimes need infinite iterations (get stuck) or demand large computational time. Due to the above factors, in this work Eq. 4 is reformulated by a differentiable approximation using a barrier method. In particular, the use of the logarithmic barrier function is used. Let $\mathbf{f_{log}}$ be the logarithmic-barrier expressed by

$$\begin{aligned} \mathbf{f_{log}}(\mathbf{u}) &= -\varphi \sum_{x\in\Omega} log c_x(u) \\ \left\{u \in \mathbb{R}^d | c_x(u) > 0 \text{ for all } x \in \Omega\right\} & \end{aligned} \tag{5}$$

where $log(\cdot)$ is the natural logarithm, $\varphi_+$ the barrier parameter that determines the impact over the function. Thus, the idea is to add $\mathbf{f_{log}}$ to the functional to be minimized in order to avoid any variable moving too close to the boundary (i.e. to zero), in consequence, it becomes a problem which can be solved using standard unconstraint methods. Thus, approximating Eq. 4 via discrete sum and adding $\mathbf{f_{log}}$ from Eq. 5, the problem to be minimized becomes

$$\begin{aligned} E_{diff}(u;\varphi) &= \{E_d(u) + \gamma E_r(u) - \varphi \mathbf{f_{log}}(u)\} \\ &= \left\{ \underbrace{\frac{1}{2}\sum_{x\in\Omega} |I_A(u(x)+x) - I_F(x)|}_{Ed} \right. \\ &\left. + \gamma \underbrace{\sum_{d=1}^{2}\sum_{x\in\Omega} |\nabla u_d(x)|}_{Er} \underbrace{- \varphi \sum_{x\in\Omega} log c_x(u)}_{\mathbf{f_{log}}} \right\} \end{aligned} \tag{6}$$

Although there are different ways to discretize the $\nabla u \in \mathbb{R}^2$ operator. In here, it is used as follows. Let $R_{int} \in \Omega$ be formed

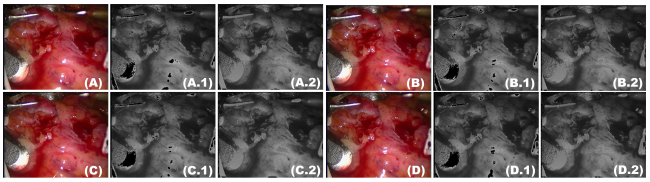


Fig. 2: After taking original sequence, (A) to (D), specular highlights are detected, (A.1) to (D.1), and the inpainting, (A.2) to (D.2), is carried out in order to retrieve the missing information.

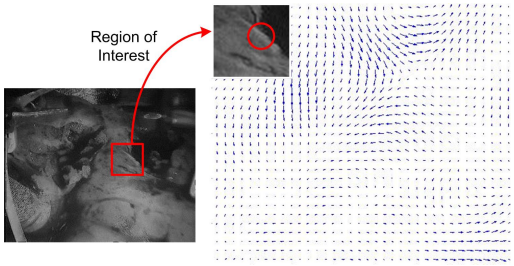


Fig. 3: Graphic of the displacement field obtained from the zone to be repaired. This zone is defined by the surgeon when the algorithm starts.

by $N*N$ pixels with $i,j$ positions, then, $\nabla u(x) = u_{i+1,j} - u_{i,j}$ $||$ $\nabla u(x) = u_{i,j+1} - u_{i,j}$ when $N < i$ $||$ $N < j$, otherwise $(N = i$ $||$ $N = j)$ $\nabla u = 0$. It must also be said that $c_x(u) = u^2$. Using the differentiable approximation expressed in Eq. 6, minimization is carried out using Newton's Method using

$$\begin{aligned} \nabla E_{diff}(u;\varphi) &= \nabla E_t(u) - \sum_{x\in\Omega} \frac{\varphi}{c_x(u)} \nabla c_x(u) \\ \nabla^2 E_{diff}(u;\varphi) &= \nabla^2 E_t(u) + \varphi \sum_{x\in\Omega} \left[ \frac{1}{c_x(u)} \nabla c_x(u) \nabla c_x(u)^T \right. \\ &\left. - \frac{1}{c_x(u)} \nabla^2 c_x(u) \right] \end{aligned} \tag{7}$$

Although various unconstraint methods can be used in combination with the log barrier, Newton's method can deal with the ill-conditioned problem given by the $\nabla^2 E_{diff}$. Additionally, using it, fast convergence can be ensured.

## IV. EXPERIMENTAL RESULTS

For validating the approach defined in Section III, simulated experimentations were conducted using a realistic data set (from The Hamlyn Centre [15]) of the heart surface affected by the respiration and the heart beat. This sequence has a duration of 60.2 sec. Tests were carried out using a PC intel Core i7-8GB RAM, and Nvidia GeForce GT 540M.

It is worth noting that specular highlights have been kept in mind in order to avoid: decreasing available information; and creating large intensity differences that produce error in the algorithm. Although the process is not explained in this work because it is not the aim, it must be emphasized that besides detection and elimination of specular highlights, image information was retrieved via inpainting (see Fig. 2).

At the beginning of the approach, identification of the region to be repaired is required (Fig. 3). Then, this region

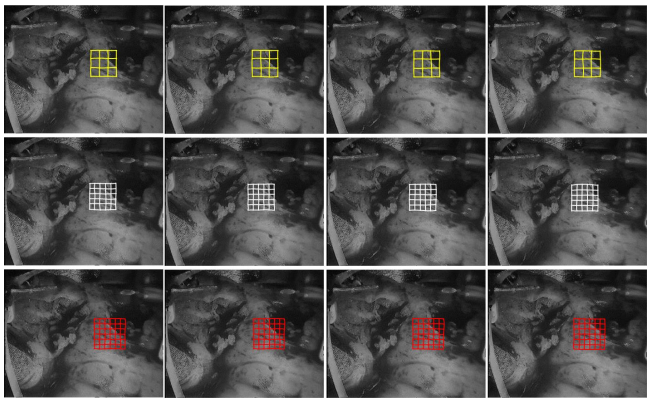

Fig. 4: Behaviour of the approach for different instants of the heart cycle using different lattice sizes. From upper row to lower row: $N = 4$, $N = 6$ and $N = 7$.

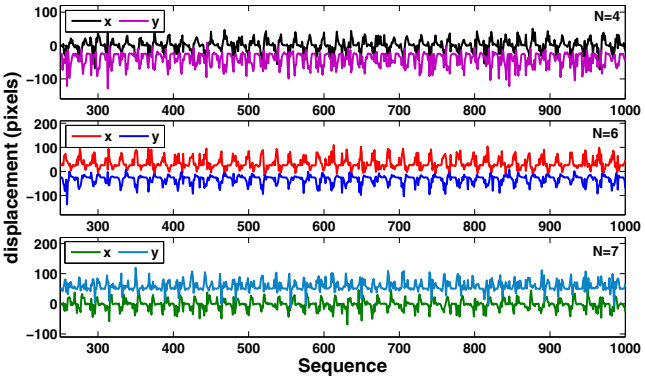


Fig. 5: Plots of the displacement are obtained from a point of interest, in both coordinates $x$ and $y$, during the heart motion using different number of control points ($N*N$).

is delimited by a grid with $N*N$ control points (lattice). In this case, experimentations were carried out using different values for $N$. However, in order to appreciate the effect of increasing $N$, values of $N = 4, 6$ and 7 were used. Results of part of the image sequence can be seen in Fig. 4 where the grid is changing with the deformation of the heart surface. In addition, the displacements, in $X-$ $Y-$ coordinates, of a point of interest to be repaired is depicted in Fig.5 during the complete sequence. As can be appreciated the more points the better approximation is obtained.

In order to validate the performance of the proposed approach, and select the best value for N, three main factors have been taken into account: Computational cost (average time per frame in sec.), number of iterations (average number per frame) and accuracy (average error in mm). Since a trade-off between efficiency and accuracy is desired and after analyzing the results of Table I, the value of N=6 has been selected. This result can be compared with the state of the art (e.g. [9], [15]).

TABLE I: Performance Analysis

| #Control Points (N*N) | Avg. Time per Frame [sec] | Avg. #Iterations per Frame | Avg. Error [mm] |
|---|---|---|---|
| 4 | 0.0035 | 15 | 0.1491 |
| **6** | **0.0054** | **15** | **0.0987** |
| 7 | 0.0073 | 18 | 0.0904 |

## V. CONCLUSIONS

In this work, the regularized version of the class $\ell_1-$ was used in order to solve the motion compensation problem in the cardiac context. Based on the results obtained from the experimentation, this approach has demonstrated its potential in terms of efficiency and robustness working under complex deformations. Moreover, it has covered the computational demands of an application oriented to work in real-time.

## ACKNOWLEDGMENT

This work is part of the project DPI2011-29660-Co4-01 MINECO and with FEDER funds EC.

## REFERENCES

[1] C. Møller and D. Steinbrchel, Off-Pump Versus On-Pump Coronary Artery Bypass Grafting, Current Cardiology Reports Springer US, pp. 1-7, 2014.

[2] J.J. Livesay, The benefits of off-pump coronary bypass: A reality or an illusion?. Texas Heart Institute Journal vol.30 num.4, pp. 258 - 260, 2003.

[3] B. Bayle, M. Joinie-Maurin, L. Barbe, J. Gangloff and M. de Mathelin, Robot Interaction control in Medicin and Surgery: Original Results and Open Problems, Computational Surgery and Dual Training, pp. 169-191, 2014.

[4] A. Lemma, A. Mangini, A. Redaelli and F. Acocella, Do cardiac stabilizers really stabilize? Experimental quantitative analysis of mechanical stabilization. Interactive CardioVascular and Thoracic Surgery, pp. 222-226, 2005.

[5] Y. Nakamura, K. Kishi and H. Kawakami, Heartbeat Synchronization for Robotic Cardiac Surgery. International Conference on Robotics and Automation, Seoul, Korea, pp. 2014-2019, 2001.

[6] T. Ortmaier, M. Groger, D.H. Boehm, V. Falk and G. Hirzinger, Motion estimation in beating heart surgery, IEEE Transactions on Biomedical Engineering, pp. 1729-1740, 2005.

[7] M. Sauve, A. Noce, P. Poignet, J. Triboulet, and E. Dombre, Three-dimensional heart motion estimation using endoscopic monocular vision system: From artificial landmarks to texture analysis. Biomedical Signal Processing and Control, pp. 199-207, 2007.

[8] R. Richa, A.P.L. Bo and P. Poignet, Towards robust 3D visual tracking for motion compensation in beating heart surgery, Medical Image Analysis, pp. 302-315, 2011.

[9] E. Bogatyrenko, P. Pascal and W.D. Hanebeck , Efficient physics-based tracking of heart surface motion for beating heart surgery robotic systems. International Journal of Computer Assisted Radiology and Surgery, Springer-Verlag, pp. 387-399, 2011.

[10] T. Ando, H. Kim, E. Kobayashi et al. , Simultaneous evaluation of wall motion and blood perfusion of a beating heart using stereoscopic fluorescence camera system. Journal in Computerized Medical Imaging and Graphics, 2014.

[11] A.I. Aviles and A. Casals, Interpolation Based Deformation Model for Minimally Invasive Beating Heart Surgery. Book Chapter IFMBE Proceedings vol.41, Springer International Publishing, 2013.

[12] M. Unser, Splines: A perfect fit for signal and image processing, IEEE Signal Processing Magazine, vol.16, no.6, pp. 22-38, 1999.

[13] J. Hadamard, Lectures on the Cauchy Problems in Linear Partial Differential Equations, New Haven Yale University Press, 1923.

[14] L. Rudin, S. J. Osher, and E. Fatemi, Nonlinear total variation based noise removal algorithms. Physica D: Nonlinear Phenomena vol. 60, 259268, 1992.

[15] D. Stoyanov, G. Mylonas, F. Deligianni, A. Darzi and G.Z. Yang, Soft-tissue Motion Tracking and Structure Estimation for Robotic Assisted MIS Procedure, Medical Image Computing and Computer Assisted Interventions, pp. 139-146, 2012.